# Ferroic phase transition in $LaEr(MoO_4)_3$

A. Hernández-Suárez[1,a)], C. Guzmán-Afonso[2], J. López-Solano[3], C. González-Silgo[3], M. E. Torres[1], N. Sabalisck[1], E. Matesanz[4] and J. Rodríguez-Carvajal[5]
[1]*Dpto. de Física Básica, Universidad de La Laguna, Avda. Astrofísico Fco. Sánchez, s/n, 38206 La Laguna, Tenerife, Spain*
[2]*Dpto. de Física Fundamental y Experimental, Electrónica y Sistemas, Universidad de La Laguna, Avda. Astrofísico Fco. Sánchez, s/n, 38206 La Laguna, Tenerife, Spain*
[3]*Dpto. de Física Fundamental II, Universidad de La Laguna, Avda. Astrofísico Fco. Sánchez, s/n, 38206 La Laguna, Tenerife, Spain*
[4]*C.A.I. Difracción de Rayos X, Universidad Complutense de Madrid, 28040 Madrid, Spain*
[5]*Institut Laue-Langevin, 6 rue Jules Horowitz, BP 156, 38042 Grenoble Cedex 9, France*

[a)] Electronic mail: anahs84@hotmail.com

The ferroic phase transition in $LaEr(MoO_4)_3$ has been analyzed for the first time. It has been confirmed that this compound undergoes a phase transition from a tetragonal system (paraelectric-paraelastic phase), with space group $P\text{-}42_1m$ [$\beta$-$Gd_2(MoO_4)_3$ averaged phase] to an orthorhombic system (ferroelectric-ferroelastic phase), with space group *Pba2* [$\beta$'-$Gd_2(MoO_4)_3$ phase] in a reversible process. This phenomenon, together with the observed demixing at high temperature has been studied using different techniques. $LaEr(MoO_4)_3$ samples have been obtained by the conventional solid-state synthesis. The thermal dependence of the crystal structure was studied by powder X-ray and neutron diffraction, following a new refining procedure in which the symmetry modes of atomic displacements from the paraelectric-paraelastic structure were analyzed. Dielectric spectroscopy measurements have confirmed the structural results, showing a very smooth phase transition. Finally, calculations within the framework of Density Functional Theory show a behavior of the lattice parameters similar to that observed in our experiments.

Key words: powder diffraction, ferroic, phase transition, dielectric spectroscopy, density functional theory.



https://doi.org/10.1017/S0885715613001127 Published online by Cambridge University Press

## I. INTRODUCTION

Rare earth molybdates with chemical composition $A_2(MoO_4)_3$ (A = Sm, Ho) are interesting because they show the ferroelectric properties of the *β'*-$Gd_2(MoO_4)_3$ structure (Jeitschko, 1972), which is known as an improper ferroelectric phase (Perez-Mato *et al.*, 2010). The ferroelectric-ferroelastic *β'*-phase of rare earth trimolybdates, with space group *Pba*2, is unique and it is related to a paraelectric-paraelastic phase unit cell with *P*-$42_1m$ space group and twice number of atoms (Perez-Mato *et al.*, 2010). Recently, Lantanum-Erbium molybdate [$LaEr(MoO_4)_3$] with the structure of *β'*-$Gd_2(MoO_4)_3$ has been investigated for its application as an infrared to visible up-conversor, as well as an efficient frequency-doubling medium for laser diode pumping (Tsukada et. al., 2009). In the present work, we present a complete dielectric and structural study of the improper ferroic phase transition. Moreover, we have also studied a possible temperature-driven phase transition above 1000 K, in which the *β*-phase should evolve toward the α-$Eu_2(WO_4)_3$ or γ-$Sc_2(WO_4)_3$ structures, depending on the ionic radii of the rare earth (Brixner et. al., 1979). Our experimental work has been complemented by a theoretical study of the structural stability of this compound.

## II. METHOD

### A. Synthesis

Lanthanum-erbium molybdate was prepared by conventional solid-state synthesis. $MoO_3$, $Er_2O_3$ and $La_2O_3$ powders (Aldrich, 99.99%) were preheated for 10 h at 923 K in the case of the molybdenum oxide, and 1173 K for the rare earth oxide. These preheated powders were weighed in stoichiometric amounts, mixed and homogenized in an agate mortar. The resulting powder was then pressed into pellets and finally sintered in air atmosphere at 1173 K for 48 h in a platinum crucible. A demixing into the phases $La_2(MoO_4)_3$ and $Er_2(MoO_4)_3$ was identified, by routine X-ray diffraction (Bergerhoff and Brown, 1987), after a heating process up to 1400 K and a quenching at room temperature.

### B. X-ray diffraction and neutron powder diffraction



https://doi.org/10.1017/S0885715613001127 Published online by Cambridge University Press

To obtain highly-accurate crystal structures, two different diffraction techniques were used. 1) X-ray diffraction was performed using a PANalytical X´Pert PRO diffractometer (Bragg-Brentano mode) at the X-ray diffraction facility of the Universidad Complutense de Madrid (Spain) with Cu $K_\alpha$ radiation. An X'Celerator detector was employed to collect X-ray diffraction data over the angular range from 5° to 120º with a step size of 0.017° $2\theta$ and a counting time of 450 seconds for the low temperature scans and 300 seconds for the high temperature measurements. Measurements were carried out, at 225, 275, 300 K in an Oxford Cryosystems Phenix cryostat; and at 300, 375, 425, 475, 500, 575 and 625K, during a heating process, under still air atmosphere, using an Anton Paar HTK 2000 camera. 2) Neutron powder diffraction was performed using the diffractometer D2B (Debye-Scherrer geometry) at the Institut Laue-Langevin (Grenoble, France) with an incident wave length of λ=1.5943(1) Å, Ge[335] monochromator, 135° take-off-angle, 5°<2θ<165° angular range, steps of 0.025° in 2θ, over 2.5 hours for each pattern, and 128 3He tubes 300 mm in height as detection system. Diffraction patterns were recorded at 225, 275, 300, 375, 425 and 475 K. Two types of patterns were extracted: a) with higher resolution, corresponding to a binning of the central equatorial zone of the detector, and b) with better counting statistics, integrating the whole detector.

### C. Dielectric Spectroscopy

Dielectric spectroscopy measurements were carried out using a Hewlett-Packard 4192, an impedance analyzer which is controlled by a computer. Measurements were recorded during a heating and cooling cycle, in the frequency range $10^2$–$10^7$ Hz with an applied voltage of 0.7 Vpp, over the temperature range 400–1000 K. The samples were in the form of pellets with surfaces coated with platinum paste, 13 mm in diameter and 1–1.5 mm in thickness.

### D. Theoretical calculations.

We have performed a density-functional-theory study of the structural stability of $LaEr(MoO_4)_3$ above the normal-conditions equilibrium volume. Calculations were performed using the plane-waves pseudopotential method with the PBEsol prescription for the exchange-correlation energy, as implemented in the VASP code (Kresse and Furthmüller, 1996). A kinetic energy cut-off of 520 eV and dense special-points grids ensured a total energy convergence of 1



https://doi.org/10.1017/S0885715613001127 Published online by Cambridge University Press

meV per formula unit. In this study we have considered two structures with distinct sites for the two rare earth cations: the *β'* phase and the orthorhombic structure with space group *Cmm*2 described in Perez-Mato *et al.*, (2010). The latter structure features the group-subgroup relationship *Pba*2 ⊂ *Cmm*2 ⊂ *P*-42$_1$*m*, and the *β* phase with space group *P*-42$_1$*m* can be considered the average of two such *Cmm*2 structures in which the La and Er atoms have been randomly distributed at the two rare earth sites. It must be stressed that in this theoretical study temperature effects are incorporated only through modifications on the volume.

## III. RESULTS AND DISCUSSION

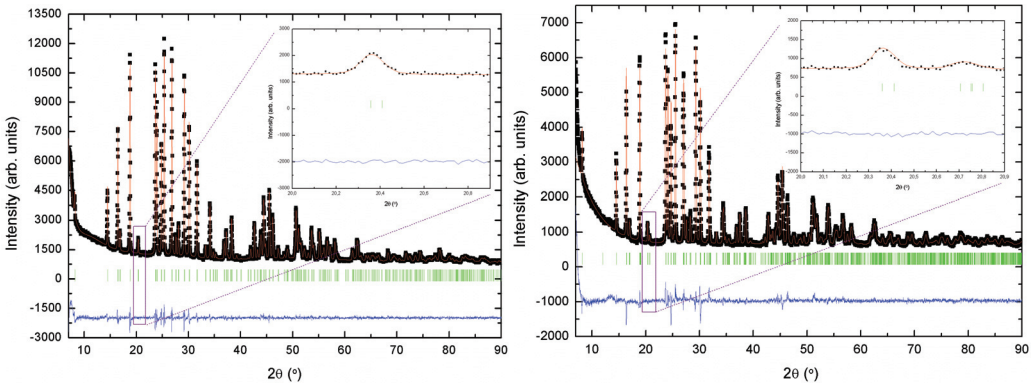



Figure 1. X-ray diffraction patterns obtained (black dots) at 625 (left) and 225 K (right) for $LaEr(MoO_4)_3$. The profile fit is shown by the red line, difference between obtained and calculated intensities is plotted by the blue line, and the vertical bars represent the expected positions of diffraction peaks. As shown in the insets, a structural phase transition takes place from the *β* paraelectric phase, stable at higher temperatures, to the *β'* ferroelectric phase, stable at lower temperatures.

We have performed a multipattern Rietveld refinement using the two neutron diffractograms and the X-ray diffractogram for each compound in the ferroelectric phase. For the paraelectric phase, only X-ray diffractograms were available, and they were refined by the Rietveld Method. The experimental profiles were modeled using a Thompson-Cox-Hasting pseudo-Voigt profile shape function and the background was modeled by a Chebyshev polynomial. We have applied a new alternative way for treating distorted structures analyzing adapted symmetry modes, using the software AMPLIMODES available at the Bilbao Crystallographic Server (Orobengoa, 2009), and the Rietveld refinement of the amplitudes of such symmetry modes (instead of the atomic coordinates), using the FullProf software suite (Rodríguez-Carvajal, 1993). AMPLIMODES determines the global structural distortion that relates the paraelectric (parent) and ferroelectric



https://doi.org/10.1017/S0885715613001127 Published online by Cambridge University Press

(distorted) phases. The ferroelectric distortion is decomposed into three distortion symmetry modes (Perez-Mato *et al.*, 2010): a primary mode corresponds to the irreducible representation $M_2$+$M_4$ associated with the point $M$ (1/2, 1/2, 0) at the border of the Brillouin zone. A secondary polar mode, at the center of the Brillouin zone, has the symmetry given by the irreducible representation $\Gamma_3$. Finally, another secondary mode given by the irreducible representation $\Gamma_1$ keeps the parent symmetry. Some of the amplitudes of such symmetry modes could be nullified, helping to reduce the number of refining parameters.

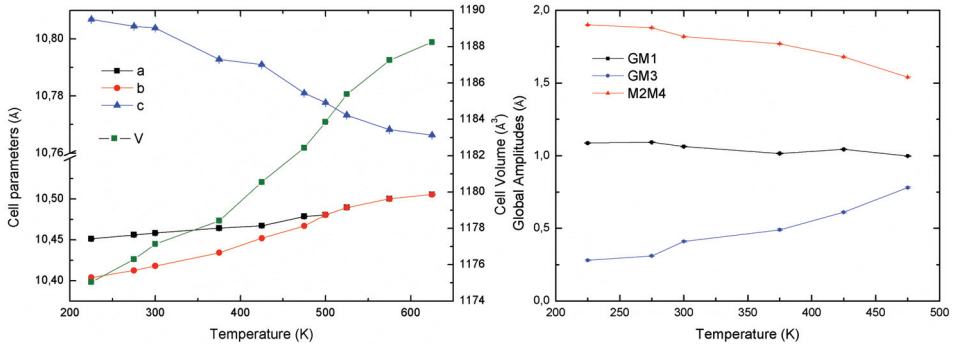



Figure 2. On the left, dependence with temperature of the cell parameters and volume. On the right, thermal dependence of the global amplitudes of the symmetry modes of each atom, in angstroms, which represent the displacement from the structure at 500 K for $LaEr(MoO_4)_3$.

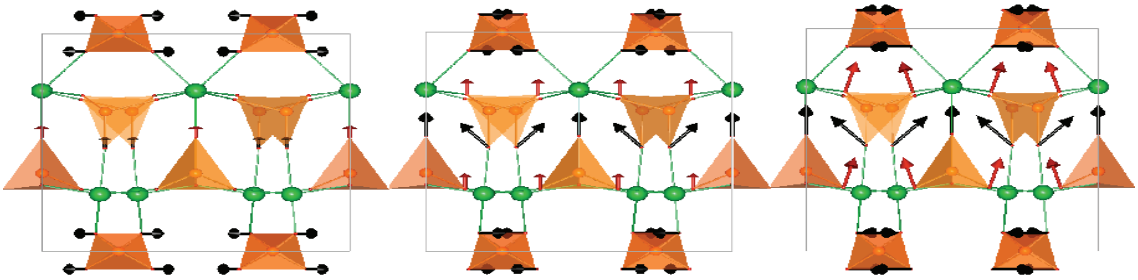


Figure 3. ***a***-axis view of the paraelectric phase of $LaEr(MoO_4)_3$ showing the oxygen displacement (with symmetry mode $\Gamma_3$) corresponding to the ferroelectric structure at 275 (left), 375 (center), 475 K (right). Black arrows indicate oxygen displacements of the RE...Mo bridges with major component in the ***c*** axis (vertical).

The results of the refinements (reliability factors and standard deviations) are consistent with similar and very recent studies on molybdates by neutron and X-ray diffraction (González-Silgo, 2010). The variation of unit-cell parameters and volume with temperature (Figure 2, left) is similar to that observed in other compounds: the ***a*** and ***b*** axes increase with increasing temperature while the ***c***-axis decreases. The latter anomalous behavior can be explained thanks to the analysis of the distortion using symmetry modes. In Figure 2 (right), we observe a correlation between the thermal dependence of the amplitudes of the $\Gamma_3$ and $M_2$+$M_4$ symmetry modes and



https://doi.org/10.1017/S0885715613001127 Published online by Cambridge University Press

the ***c*** cell parameter. The symmetry mode $M_2$+$M_4$ decreases with increasing temperature and its direction is constant. However the symmetry mode $\Gamma_3$ generally increases with increasing temperature and its direction changes. The dependence on heating of the symmetry modes $M_2$+$M_4$ and $\Gamma_3$ are represented by scaled arrows too, which correspond to the oxygen displacements from the paraelectric to the ferroelectic phase (Figure 3). The anomalous behavior in the cell parameter ***c*** can be explained by the shortening of the RE...Mo non-bonding distances parallel to the ***c*** axis, and of their angles through the displacements of the binding oxygen with $\Gamma_3$ symmetry (Figure 3).

Dielectric spectroscopy measurements (Figure 4, left) are consistent with our experimental results. We have not detected a clear phase transition as in other compounds with the *β'*-phase (Brixner *et. al.*, 1979). Only in the conductivity (imaginary part of the dielectric constant) it is possible to see "slight changes" around 500 K, which are compatible with the structural modification observed in X-ray experiments, but we cannot assure the existence a ferroelectric-paraelectric phase transition.

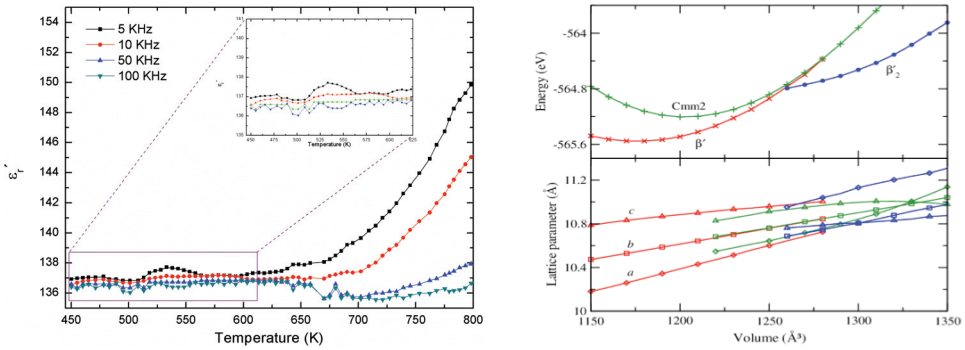



Figure 4. On the left, dependence of the real part of complex dielectric permittivity with temperature for different frequencies. On the right, results of our theoretical study: the upper panel shows energy-volume curves for the *β'* (red), *Cmm2* (green), and *β'*$_2$ (blue) structures; the lower panel shows the volume dependence of the ***a*** (diamonds), ***b*** (squares) and ***c*** (triangles) lattice parameters of the structures in the upper panel (color code is kept unchanged between both panels).

The structures obtained for the ferroelectric phase are consistent with our theoretical results, in which the La and Er atoms can be interchanged between the two non-equivalent sites. In our theoretical study we find that the *β'* phase evolves into a structure with space group *Cmm*2 as the volume increases (Figure 4). In this latter structure, the La and Er atoms can be also interchanged. The existence of a polar phase at high volume/temperature is compatible with the



https://doi.org/10.1017/S0885715613001127 Published online by Cambridge University Press

dielectric measurements, in which a very smooth *Pba*2-to-*Cmm*2 phase transition is expected to develop. The dependence with the volume of the theoretical cell parameters of the *β'* and *Cmm*2 phases is similar to the experimentally-observed behavior under temperature. The theoretical ***c*** cell parameter decreases after reaching a maximum value, and the ***a*** and ***b*** parameters converge. According to our calculations, at very high volumes a modification of the *β'* phase (labeled $\beta'_2$ in Figure 4), with noticeably different lattice parameters, becomes energetically favorable.

As a closing remark, we note that the high-temperature demixing towards separate $La_2(MoO_4)_3$ and $Er_2(MoO_4)_3$ phases (with space groups *C*2/*c* and *Pbcn*, respectively) is compatible with the behavior observed in other *β*-phases after decomposition (Brixner et. al., 1979), even though in the present case we have two rare earths with very different ionic radii.

## IV. CONCLUSION

As part of a thorough and comprehensive study on the behavior of ferroelectric phases using both experimental measurements (González-Silgo, 2010) and theoretical simulations, we have studied for the first time lanthanum-erbium molybdate. A very smooth phase transition from the high-temperature *β* paraelectric phase to the low-temperature *β'* ferroelectric phase has been observed at ~500 K by X-ray and dielectric spectroscopy. The thermal dependence of the ferroelectric-ferroelastic structure obtained in the X-ray and neutron diffraction experiments has been explained. The theoretical evolution of the lattice parameters is similar to that observed in our experiments. We have also observed a demixing toward the phases $La_2(MoO_4)_3$ and $Er_2(MoO_4)_3$ at high temperature. High-temperature ferroelectric hysteresis and neutron diffraction experiments should be performed in order to check the stability of the possible polar *Cmm*2 phase (or of another *β'*-like phase, as predicted in our *ab initio* calculations), instead of the paraelectric *β*-phase.

## ACKNOWLEDGMENTS

The authors are grateful the Ministerio de Ciencia e Innovación of Spain (MICCIN) under The National Program of Materials (MAT2010-21270-C04-02/03), the Consolider-Ingenio 2010



https://doi.org/10.1017/S0885715613001127 Published online by Cambridge University Press

Program (MALTA CSD2007-0045), and to EU-FEDER funds for their financial support. J. López-Solano gratefully acknowledges access to the computational resources of the MALTA Cluster Computer (Universidad de Oviedo) and the Red Española de Supercomputación. C. Guzmán-Afonso wishes to thank ACIISI and FSE for a fellowship.

Bergerhoff, G. and Brown, I. D. (**1987**). *Crystallographic Databases*, Allen F. H. *et al*. (Hrsg.) International Union of Crystallography, Chester).

Brixner L. H., Barkley J. R. and Jeitschko W. (**1979**). *Handbook on the Physics and Chemistry of Rare Earth* (Amsterdam: North-Holland).

González-Silgo C., Institut Laue-Langevin D2B, Experimental Report of the Proposal 5-23-626 (accepted in 2010).

Jeitschko, W. (**1972**). "A Comprehensive X-ray Study of the Ferroelectric-Ferroelastic and Paraelectric-Paraelastic Phases of $Gd_2(MoO_4)_3$," Acta Crystallogr., Sect. B: Struct. Crystallogr. Cryst. Chem. **28**, 60-76.

Kresse G. and Furthmüller J. (**1996**), "Efficient iterative schemes for *ab initio* total-energy calculations using a plane-wave basis set," Phys Rev. B **54**, 11169-11186.

Orobengoa D., Capillas C., Aroyo M. I. and Pérez-Mato J. M. (**2009**). "AMPLIMODES: symmetry-mode analysis on the Bilbao Crystallographic Server," J. Appl. Crystallogr. **42**, 820-833.

Perez-Mato, J. M., Orobengoa, D. and Aroyo, M. I. (**2010**). "Mode crystallography of distorted structures," Acta Crystallogr., Sect. A : Found. Crystallogr. **66**, 558-590.

Rodríguez-Carvajal, J. (**1993**). "Recent advances in magnetic structure determination by neutron powder diffraction," Physica B **192**, 55-69.

Tsukada Y, Honma T and Komatsu T. (**2009**). "Self-organized periodic domain structure for second harmonic generations in ferroelastic $\beta'$-$(Sm,Gd)_2(MoO_4)_3$ crystal lines on glass surfaces," Appl. Phys. Lett. **94**, 041915.



https://doi.org/10.1017/S0885715613001127 Published online by Cambridge University Press